# Remote Sensing Technologies in the Search for Rare Metal Deposits in Eastern Kazakhstan

Marzhan Ye. Rakhymberdina<sup>1\*</sup>, Yerkebulan T. Bekishev<sup>1</sup>, Roman Shults<sup>2</sup>, Baytak Apshikur<sup>1</sup>, Yevgeniy Grokhotov<sup>1</sup>, Zhanna A. Assylkhanova<sup>1</sup>, Marzhan M. Toguzova<sup>1</sup>, Almagul K. Abdygaliyeva<sup>1</sup>

<sup>1</sup>D. Serikbayev East Kazakhstan Technical University, Ust-Kamenogorsk, Kazakhstan – MRahymberdina@edu.ektu.kz, YBekishev@edu.ektu.kz, BApshikur@edu.ektu.kz, info@geosat.biz, ZhAssylkhanova@edu.ektu.kz, MToguzova@edu.ektu.kz, AAbdygolieva@ektu.kz

Keywords: Remote Sensing, Rare Metals, Multispectral Image, Satellite Data, Deposit.

#### Abstract

The article explores the potential of remote sensing (RS) applications for identifying patterns of rare metal mineralization in the studied area of Eastern Kazakhstan. An analysis of the technical parameters related to RS data is conducted to highlight the structural and lithological features, which allows for a deeper understanding of the geological environment and the region's potential resources. The research is based on multispectral satellite data obtained within potentially promising magmatogenic ore systems. The authors emphasize the identification of areas with a high probability of discovering rare metal mineralization, which can play a crucial role in the exploration and development of deposits. A key element of the study is the analysis of spectral characteristics of rare metal pegmatites and their constituent minerals, enabling the establishment of their unique signatures in the spectral data. The article also discusses the methods for processing and interpreting multispectral images, which are essential for accurately identifying minerals and assessing their distribution. Modern machine learning techniques are applied in the research, significantly increasing the efficiency of data analysis and allowing for the automation of mineral identification and classification processes. As a result, meaningful conclusions are drawn about the region's potential for rare metal extraction, opening new prospects for further research and practical applications in geological exploration.

#### 1. Introduction

The mining industry is a key sector of the economy in many countries worldwide. It serves, first and foremost, as an instrument of national security, as well as a source of employment and income for a significant part of the population. According to (Ericsson, Löf, 2019), the successful implementation of geological exploration activities determines the future dynamics of mining development and lays the foundation for increased mineral production within the next 10-15 years.

A review of key trends in the mining industry shows that over the next 5-10 years, the global sector will undergo significant transformations driven by global consumer and technological developments. Rising demands for higher product quality are increasing the need for innovation, including artificial intelligence (AI), machine learning (ML), remote control, and other.

The introduction of remote methods, machine learning and artificial intelligence into Kazakhstan's mining and geological industry to optimise mineral exploration processes and manage ore deposit recognition is a relevant and promising area of development for the geological exploration industry, which makes it possible to increase the efficiency and accuracy of research, optimise the planning and design of work, improve the prediction of ore occurrences and control the results of research. When considering the specifics and role of the mining industry, it is necessary to note the following global problems facing society: depletion of profitable mineral reserves due to large volumes of extraction, complex and expensive geological conditions for exploration and development of deposits, a growing demand for rare and rare-earth metals in countries with high-tech industries, and intensifying competition between countries for mineral resources.

Rare metals are a group of chemical elements with unique properties that are widely applied in high-tech industries such as emerging energy technologies, nuclear power, aerospace, and others, which makes them critical strategic resources linked to economic security and national defense (Li et al., 2020). These metals are often characterized by low concentrations in the Earth's crust or by the complexity of their extraction and processing. To date, more than 60 types of rare metals have been identified. Among the most well-known are lithium (Li), beryllium (Be), and tantalum (Ta). Technological progress and the recent surge in demand for electronics and electric vehicles have triggered renewed global interest in these metals. For instance, according to the U.S. Geological Survey, a decade ago the primary market for lithium consumption was ceramics production, which accounted for one-third of total demand. Today, this share has decreased to just 7%, without a reduction in absolute consumption, while the dominant consumer has become the battery industry, which now represents more than 80% of total demand (Lithium Statistics and Information, 2025). A similar trend can be observed in the market for other rare metals. Given the growth in metal prices and consumption, it is necessary to actively conduct geological research to expand the country's mineral resource base.

The Republic of Kazakhstan possesses considerable reserves of rare-metal mineral resources. Currently, 37 deposits and about 500 ore occurrences of rare metals and rare elements have been identified. However, the discovery of new deposits and the exploration of rare metals remain stagnant. For example, since the 1970s, no new deposits associated with rare-metal pegmatites have been discovered. In the 1990s, the extraction of rare-metal ores was almost completely halted and has not been resumed to date (Hunt, 1977).

Eastern Kazakhstan is considered the primary rare metal and rare earth geological province, characterised predominantly by tintantalum-niobium and zirconium-tantalum-niobium

<sup>&</sup>lt;sup>2</sup> Interdisciplinary Research Center for Aviation and Space Exploration, King Fahd University of Petroleum and Minerals, 34463 Dhahran, Saudi Arabia – roman.shults@kfupm.edu.sa

mineralisation. All known industrial deposits and major ore occurrences have been identified in surface outcrops within the Kalba-Narym rare metal belt. However, since the 1970s, no new tantalum deposits associated with rare-metal pegmatites have been discovered, suggesting that the region's easily identifiable reserves have essentially been exhausted.

The detection of mineral deposits using remote sensing methods has its specific features, as mineral reflectance spectra are generally unique and certain minerals exhibit distinct absorption and reflection bands corresponding to remote sensing image wavelengths. The primary factors influencing the spectral characteristics of minerals and rocks are limited to a few key elements: iron, which produces electronic transitions, and water, hydroxyl ions, and carbonates, which are responsible for vibrational transitions. In the near-infrared range, absorption features are primarily caused by iron (700-900 nm), while in the shortwave infrared range, spectral variations are attributed to water and hydroxyl ions. For instance, absorption features at approximately 1140 nm, 1400 nm, and 1900 nm indicate the presence of water within the mineral structure (Hunt, 1977).

The identification of spectral signatures of pegmatites based on existing spectral libraries appears to be unfeasible. This is due to the fact that the spectral signature of each rock type represents a combination of the reflectance and absorption characteristics of its constituent minerals, as well as their relative proportions. For example, the authors of (Gao et al., 2020) note that rare-metal pegmatites exhibit reflectance in the visible-near infrared (VNIR) region (0,55-060 μm), while the authors of (Cardoso-Fernandes et al., 2021) indicate that rocks within the same range may instead absorb electromagnetic radiation. In addition, the presence of hydrothermally altered rocks can cause shifts or anomalies in certain spectral ranges. In the work (Wang et al., 2017), remote sensing methods are used to identify volcanogenic massive sulphide and hydrothermal deposits in the Honghai district (China), remote sensing methods are used, where exploration targets are identified based on a combination of geological factors from remote sensing and the integration of multiple change factors obtained from remote sensing with different weighting coefficients. The Google Earth Engine (GEE) plays an important role in this research, providing access to a huge archive of satellite images, in particular to archived multispectral images from the Landsat and Sentinel 2 satellite series, and other geospatial data, and offering tools for analysing this data using high-performance computing and machine learning capabilities (Lindsay et al., 2022, Zhao et al., 2021).

The mineral composition of pegmatites is well-documented from archival data; however, since rocks represent a dense mixture in which constituent minerals are closely interlinked, it is not theoretically feasible to construct a spectral signature solely on the basis of reference spectra of individual minerals.

The purpose of this work is to analyse the possibilities of using remote sensing methods, processing and interpreting multispectral images for accurate identification of minerals and assessment of their distribution.

#### 2. Material and Methods

# 2.1 Research area

The research area, the Kalba–Narym metallogenic (ore) zone, is located within the East Kazakhstan region of the Republic of Kazakhstan. Geographically, the ore zone lies on the southwestern margin of the Altai Mountains. It forms part of the Greater Altai together with the Altai, Zharma-Saur, and Western Kalba ore districts (D'yachkov B.A. et al., 2021). The metallogenic zone extends for more than 500 km in a northwestern direction, with a width ranging from 20 to 50 km.

It borders the Russian Federation to the northwest and the People's Republic of China to the southeast, while the Ertis gravel district lies to the northeast and the Terekty anomaly to the southwest. All known deposits and ore occurrences in this area are confined to granitoid complexes of varying ages and compositions (Figure 1).

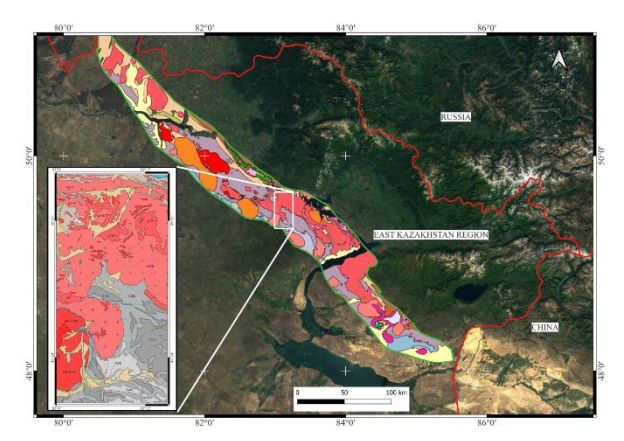


Figure 1. Kalba-Narym ore belt with indication of the Asubulak ore field

The Asubulak deposit (pegmatite massif) is part of the Kalba–Narym metallogenic zone. The pegmatite massif is located in the central part of the Kalba-Narym zone, at the intersection of three faults, within the granite intrusion of the Kalba Complex of Permian age. Across the area, aplite, aplite-pegmatite, pegmatite, and rare-metal pegmatites are widespread. The rare-metal pegmatites occur within the first-phase granites (Khromykh S.V. et al., 2020).

### 2.2 Initial data

As the primary data sources, satellite imagery from the Landsat-8 and Sentinel-2 missions was used. Both satellite families include shortwave infrared (SWIR) bands, which are essential for geological mapping and for enhancing the contrast of geological features.

From Landsat-8, the USGS Landsat 8 Level 2, Collection 2, Tier 2 dataset was utilized. This dataset provides atmospherically corrected surface reflectance and land surface temperature derived from the Landsat 8 OLI/TIRS sensors. The imagery includes five bands in the visible and near-infrared (VNIR) range and two bands in the shortwave infrared (SWIR) range, processed to surface reflectance orthorectified products, as well as one band in the thermal infrared (TIR) range, processed to orthorectified surface temperature. In addition, it contains intermediate bands used in the generation of ST products, along with quality assessment bands.

Landsat 8 surface reflectance (SR) products are generated using the Land Surface Reflectance Code (LaSRC). All Collection 2 surface temperature (ST) products are derived using the single-channel algorithm jointly developed by the Rochester Institute of Technology (RIT) and the Jet Propulsion Laboratory (JPL) of the National Aeronautics and Space Administration (NASA). The acquired data fragments are assembled into overlapping "scenes" of approximately 170 × 183 km using a standard reference grid (Google Earth Engine, 2024).

Sentinel-2 imagery was used in the form of Level-2A products from the Harmonized Sentinel-2 MSI (MultiSpectral Instrument) dataset, which are atmospherically corrected and therefore do not require additional preprocessing. Sentinel-2 is a wide-swath, high-resolution multispectral imaging system designed for

terrestrial monitoring under the Copernicus program, including vegetation, soil, and water cover assessment, as well as observations of inland waterways and coastal areas.

Sentinel-2 L2 data were downloaded from the Copernicus Data Space Ecosystem (CDSE) and processed using sen2cor.

The datasets contain 12 spectral bands in UINT16 format, representing surface reflectance (SR) scaled by a factor of 10000 (unlike Level-1 data, Band 10 is not included). Several additional bands specific to Level-2 products are also available (S2Applications, 2025).

#### 2.3 Data processing

The collection and processing of remote sensing data was carried out on the Google Earth Engine (GEE) platform (Zhao et al., 2024).

The processing of Landsat-8 images includes:

- Landsat 8 data selection: the LANDSAT/LC08/C02/T1\_L2 satellite data collection provided by Google Earth Engine was used. This collection contains pre-calibrated images with high-precision radiometric and geometric calibration, as well as atmospheric correction;
- Filtering of the data by region and acquisition date to extract the region of interest (roi) was carried out using the filterBounds function, which allows the selection of images covering the specified area. The acquisition dates were restricted to the period from June 1, 2020 to September 1, 2024 using the filterDate method. Following this filtering, the first suitable image with the lowest cloud coverage was selected using the .first() method, which simplifies the process of image selection within the given time interval;
- Image clipping was performed using the .clip(roi) function, which allows trimming of the imagery to the boundaries of the region of interest. This ensures precise correspondence of the data to the specified area, facilitating more convenient subsequent processing and visualization;
- Data transformation was performed using the .toInt16() method, which converted the imagery into the Int16 format, thereby reducing data volume and optimizing computational efficiency. For the visualization of Sentinel-2 imagery, analogous techniques and JavaScript codes in Google Earth Engine were applied.

To identify differences between the spectral properties of rocks, the Random Forest machine learning method was applied. Random Forest is an ensemble algorithm that utilizes multiple decision trees. The dataset for machine learning was derived from a shapefile with an attribute table. Based on archival geological maps and field observations, 80 points were selected and georeferenced on a Sentinel-2A satellite image. Each point was assigned a lithology class with numerical values (sedimentary rocks – 1, granites – 2, pegmatites – 3). In addition, using the Sample Raster Values plugin, spectral reflectance values for each point were extracted across all 12 Sentinel-2A bands.

The model training with Random Forest was performed in Python using the Pandas and NumPy libraries.

## 3. Results and discussion

The downloaded satellite images were imported into QGIS software (version 3.36), which provides a more convenient environment for performing cartographic operations. To enhance the contrast between geological features, techniques such as RGB band combinations and band ratios were applied.

RGB combinations involve the creation of false-color composites based on the known spectral properties of rocks and minerals relative to selected spectral bands. Each chosen band is assigned to a specific color channel (red, green, or blue), and depending on the reflectance characteristics, the surface features are displayed in new contrasting colors.

The band ratio technique involves enhancements obtained by dividing the digital number (DN) values of one spectral band by the corresponding values of another band. This method is particularly useful for highlighting specific materials that may not be visible in unprocessed bands. In addition, it helps to reduce shading and topographic effects, making it especially suitable for complex terrains (Bekishev et al., 2024).

Based on a review of the relevant literature, well-established band combinations and ratios were selected for this study (Table 1).

RGB combinations			
Landsat-8	Sentinel-2	Features	Authors
2-5-7		Iron oxides and clay minerals	Ali and Pour (Ali and Pour, 2014)
5-6-7	11-4-12 8-12-3	Lithological contrasts	Mwaniki et al. (Mwaniki et al., 2015)
5-7-3	8-12-3	Altered rock formations	Bodruddoza and Fujimitsu (Bodruddoza, Fujimitsu, 2012
Aspect ratio			
6/7	11/12	Altered rocks	Sabins (Sabins, 1999)

Table 1. RGB combinations and band ratios.

At the Akhmetkino deposit site, Sentinel-2 and Landsat-8 imagery, after processing, clearly revealed the contours of anthropogenic impacts as well as exposures of bedrock at the surface. On the Sentinel-2 scene, when using the 8-12-3 band combination (Figure 2b), the rocks appeared in dark gray, while in the 8-11-12 combination they appeared in blue (Figure 2c). A similar result was obtained after processing Landsat-8 imagery (Figure 3b, c). The color differentiation distinctly separates bedrock from the surrounding features. Band ratio analysis further delineates geological objects based on differences in the digital values of pixels across the selected bands. Bright pixels on the Sentinel-2 scene (Figure 2d) highlighted these variations, as did the 6/7 band ratio from Landsat-8 (Figure 3d). However, Landsat-8 imagery has a lower spatial resolution (30 m), which reduces the interpretability of small-scale features.

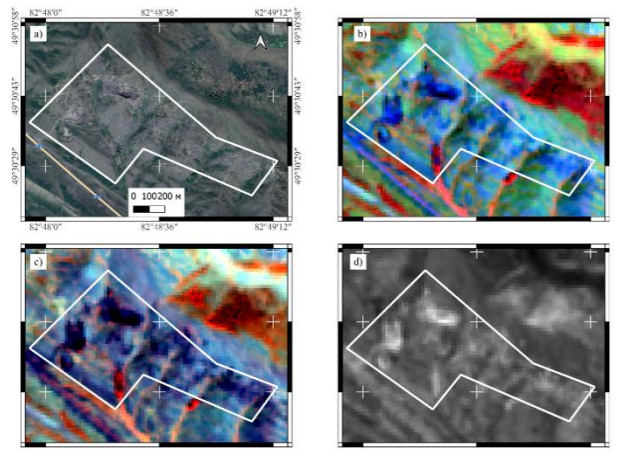


Figure 2. Targyn area (Akhmetkino deposit): a) satellite image in natural colors; b) Sentinel-2 image, band combination 8-12-3; c) Sentinel-2 image, band combination 8-11-12; d) Sentinel-2 image, band ratio 11/12.

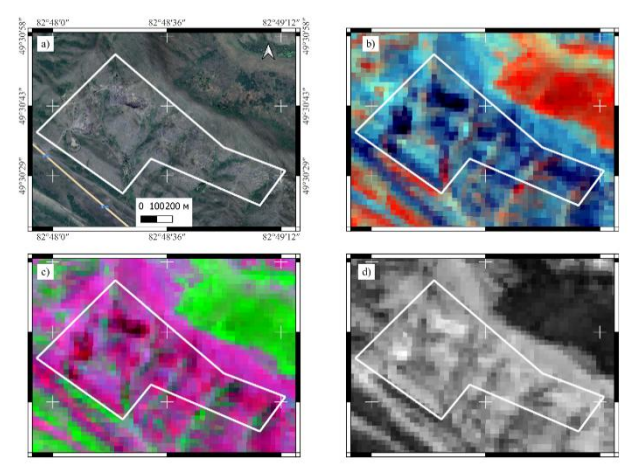


Figure 3. Targyn area (Akhmetkino deposit): a) satellite image in natural colors; b) Landsat-8 image, band combination 5-6-7; c) Landsat-8 image, band combination 2-5-7; d) Landsat-8 image, band ratio 6/7.

The study area near Zhantas village did not yield significant results, as reed thickets surrounding the artificial reservoir obscured the geological features. Consequently, this site produced spectral confusion with other types of vegetation (Figure 4b, c; Figure 5b, c). The band ratio technique using Sentinel-2 shortwave infrared bands also showed no meaningful results due to the absence of exposed geological formations in the area (Figure 4d). A similar approach applied to Landsat-8 imagery likewise did not reveal any spectral anomalies (Figure 5d).

Lake Zharkynkol and the former quarry are clearly visible in the images, as geological features have high reflectance in the SWIR range. In all combinations and ratios of Landsat-8 and Sentinel-2, the pixels of the man-made area acquired characteristic colours and brightness, which are visually easy to distinguish from other cartographic objects (Figures 6, 7).

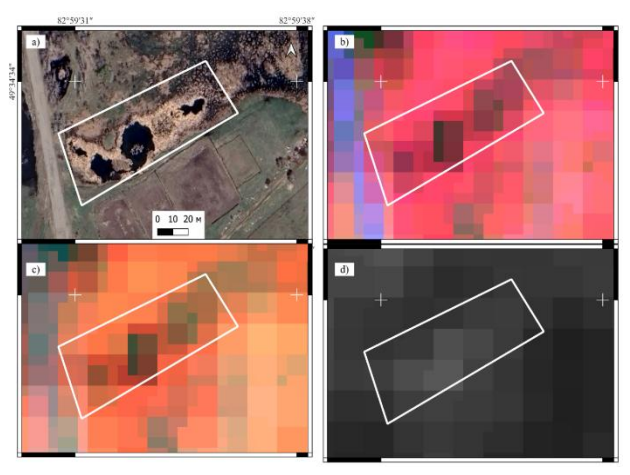


Figure 4. Zhantas village area: a) satellite image in natural colors; b) Sentinel-2 image, band combination 8-12-3; c) Sentinel-2 image, band combination 8-11-12; d) Sentinel-2 image, band ratio 11/12.

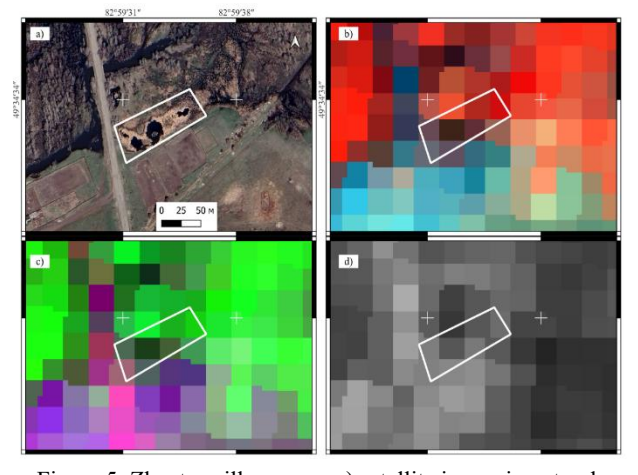


Figure 5. Zhantas village area: a) satellite image in natural colors; b) Landsat-8 image, band combination 5-6-7; c) Landsat-8 image, band combination 2-5-7; d) Landsat-8 image, band ratio 6/7.

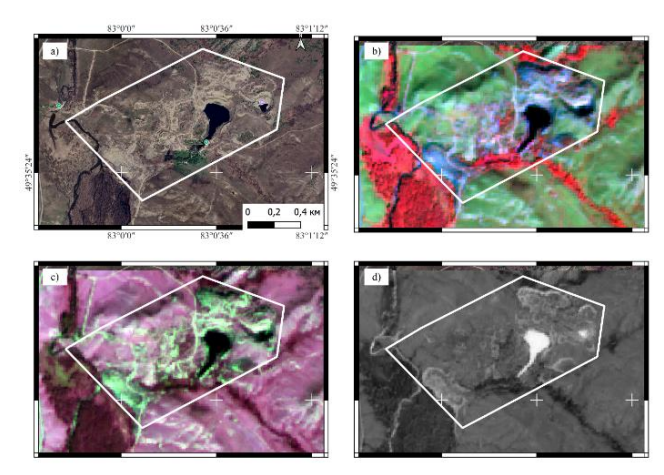


Figure 6. Zharkynkol Lake area: a) satellite image in natural colors; b) Sentinel-2 image, band combination 8-12-3; c) Sentinel-2 image, band combination 11-4-2; d) Sentinel-2 image, band ratio 3/8.

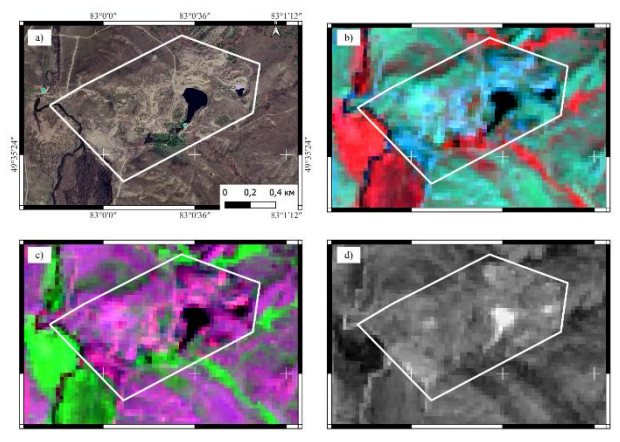


Figure 7. Zharkynkol Lake area: a) satellite image in natural colors; b) Landsat-8 image, band combination 5-7-3; c) Landsat-8 image, band combination 2-5-7; d) Landsat-8 image, band ratio 6/7.

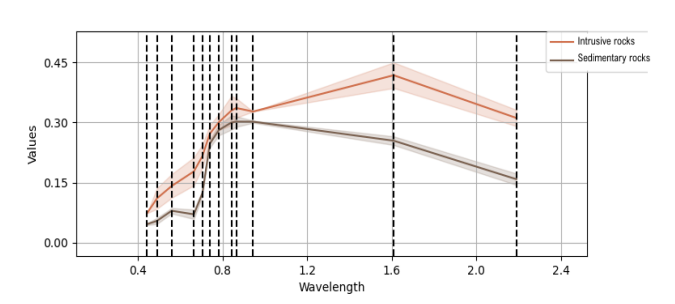


Figure 8. Spectral reflectance curves for intrusive and sedimentary rocks.

The visual distinction in lithological mapping is primarily explained by the different reflectance properties of rocks. Figure 8 shows the averaged spectral reflectance curves derived from Sentinel-2A data for intrusive rocks (granites, pegmatites) and sedimentary rocks (clay shales). It is evident that intrusive rocks (orange curve) exhibit higher reflectance values across almost the entire spectral range  $(0.4-2.2~\mu m),$  with a pronounced increase in the near-infrared region (around 1.6  $\mu m).$  In contrast, sedimentary rocks (black curve) are characterized by lower reflectance and a smoother spectral trend.

The key differences are as follows:

- 1. Visible range  $(0.4-0.7~\mu m)$ . Intrusive rocks exhibit higher reflectance due to the light color of their constituent minerals (quartz, feldspar, and muscovite in pegmatites). In contrast, sedimentary clay shales appear darker, as they contain organic matter and iron-bearing compounds, which reduce reflectance.
- 2. Red edge (around  $0.7-0.8~\mu m$ ). Granites and pegmatites show a more pronounced increase in reflectance, which is associated with their mineralogical composition and lower concentrations of absorbing impurities. In clay shales, the transition is less pronounced.
- 3. Near-infrared (1,6  $\mu m$ ). Intrusive rocks reach their maximum reflectance values, whereas sedimentary rocks remain at relatively low levels. This is due to differences in texture: granites and pegmatites consist of large-grained minerals with high reflectivity, while shales consist of a fine-grained clay matrix that better absorbs radiation.
- 4. Mid-infrared range  $(2,1-2,2~\mu m)$ . In this region, reflectance decreases for both groups, but intrusive rocks still maintain higher values. For shales, absorption features become more pronounced, associated with the presence of hydrated minerals

such as kaolinite and montmorillonite. Granites and pegmatites are rich in quartz and feldspar, which have relatively high reflectance. Clay shales contain dark minerals, iron, and organic matter, resulting in reduced albedo. The coarse-grained texture of intrusive rocks enhances light scattering, while the fine-grained and compact structure of shales promotes absorption. Sedimentary clay-rich rocks contain minerals that actively absorb in the near- and mid-infrared ranges (e.g., OH-group and  $\rm H_2O$  absorption bands), leading to a further decline in reflectance. Overall, the observed differences in spectral curves are primarily controlled by mineralogy, color, and texture of the rocks, which provides a basis for using satellite imagery to map and classify intrusive and sedimentary complexes.

Supervised classification using the Random Forest method was performed with class balancing and hyperparameter tuning. As a result, the model achieved a moderately average accuracy in distinguishing rock types (Figure 9).

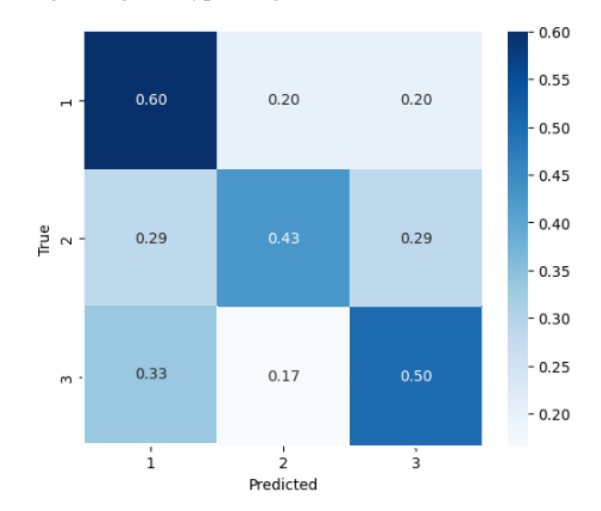


Figure 9. Confusion Matrix

Figure 9 presents the confusion matrix illustrating the classification accuracy of the model. The Y-axis (True) represents the actual class labels (1 – sedimentary rocks, 2 – granites, 3 – pegmatites), while the X-axis (Predicted) shows the labels assigned by the model. Cells - the percentage of objects that fall into the corresponding category.

The model identifies sedimentary rocks (clay shales) with an accuracy of 60%, but misclassifies them into other categories in about 20% of cases. The classification accuracy for granites and pegmatites is 43% and 50%, respectively, although some pixel-level confusion remains. Overall, the model's accuracy can be considered moderate. Apparently, relatively low spatial resolutions of images do not yield high recognition results.

### 4. Conclusion

This article examined the potential of using Landsat-8 and Sentinel-2 satellite data for mineralogical mapping and creating contrast maps between different types of rocks. Based on the analysis of RGB band combinations and the application of band ratio techniques, attempts were made to identify rare-metal pegmatites and to distinguish them from granites and host sedimentary rocks.

The possibility of using machine learning for automatic detection and mapping of rocks was also considered.

The results obtained showed that it is possible to reliably distinguish between intrusive rocks and sedimentary complexes, confirming the effectiveness of medium-resolution satellite data for regional geological mapping tasks. However, the small size

of pegmatite bodies, as well as the limited spatial and spectral resolution of Sentinel-2 and Landsat-8 images, did not allow for their detailed identification.

In the future, to improve the accuracy of mineralogical mapping and the identification of small objects, it is advisable to use ultrahigh spatial resolution data, such as WorldView-3 images, as well as hyperspectral survey materials. This will allow for more reliable differentiation between pegmatite bodies and their mineralogical features, opening up new prospects for the search for and evaluation of rare metal deposits.

#### Acknowledgements

This research was supported by project IRN BR24992854 "Development and implementation of competitive science-based technologies to ensure sustainable development of mining and metallurgy industry East Kazakhstan region", funded by the Science Committee of the Ministry of Science and Higher Education of the Republic of Kazakhstan.

### References

Ali A., Pour A.B., 2014: Lithological mapping and hydrothermal alteration using Landsat 8 data: a case study in ariab mining district, red sea hills, Sudan. *International Journal of Basic and Applied Sciences*. 3, 199. doi:10.14419/ijbas.v3i3.2821

Bekishev Ye., Rakhymberdina M., Levin E., Assylkhanova Zh., Kapasov A., 2024: Creating of a geological GIS database of Eastern Kazakhstan using the Kalba-Narym Zone as an example// Asian Conference on Remote Sensing (ACRS 2024). https://acrs-aars.org/proceeding/ACRS2024/AB0282.pdf

Bodruddoza M., Fujimitsu Y., 2012: Mapping hydrothermal altered mineral deposits using Landsat 7 ETM+ image in and around Kuju volcano, Kyushu, Japan. *Journal of Earth System Science*. 121, 1049-1057. https://doi:10.1007/s12040-012-0211-9

Cardoso-Fernandes J., Silva J., Perrotta M., Lima A., Teodoro A., Ribeiro M., Dias F., Barrès O., Cauzid J., & Roda-Robles E., 2021: Interpretation of the Reflectance Spectra of Lithium (Li) Minerals and Pegmatites: A Case Study for Mineralogical and Lithological Identification in the Fregeneda-Almendra Area. *Remote Sensing.* 13(18), 3688. doi.org/10.3390/rs13183688

D'yachkov, B., Bissatova, A., Mizernaya, M., Khromykh, S., Oitseva, T., Kuzmina, O., Aitbayeva, S., 2021: Mineralogical tracers of gold and rare-metal mineralization in eastern Kazakhstan. *Minerals*. 11(3), 253. https://doi.org/10.3390/min11030253.

Ericsson, M., Löf, O., 2019: Mining's contribution to national economies between 1996 and 2016. *Gornaya promyshlennost = Russian Mining Industry*. (6), 84–93. doi.org10.30686/1609-9192-2019-6-84-93

Gao Y., Bagas L., Li K., Jin M., Liu Y., & Teng J., 2020: Newly Discovered Triassic Lithium Deposits in the Dahongliutan Area, NorthWest China: A Case Study for the Detection of Lithium-Bearing Pegmatite Deposits in Rugged Terrains Using Remote-Sensing Data and Images. *Frontiers in Earth Science*. 8, 591966. doi.org/10.3389/feart.2020.591966

Google Earth Engine, 2024. https://developers.google.com/earth-

eng/datasets/catalog/LANDSAT LC08 C0 T2 L2 (11 November 2024)

Hunt G.R. 1977: Spectral signature of particulate minerals in the visible and near infrared. *Geophysics*. 42(3), 501–513. https://www.sci-hub.ru/10.1190/1.1440721

Khromykh, S., Oitseva, T., Kotler, P., D'yachkov, B., Smirnov, S., Travin, A., Agaliyeva, B., 2020: Rare-metal pegmatite deposits of the Kalba region, Eastern Kazakhstan: Age, composition and petrogenetic implications. *Minerals*. 10(11), 1017. https://doi.org/10.3390/min10111017

Li, H., Xu F., Li Q., 2020: Remote sensing monitoring of land damage and restoration in rare earth mining areas in 6 counties in southern Jiangxi based on multisource sequential images. *Journal of Environmental Management*. 267(2), 110653. doi.org10.1016/j.jenvman.2020.110653

Lindsay E., Frauenfelder R., Rüther D., Nava L., Rubensdotter L., Strout J., Nordal S., 2022: Multi-Temporal Satellite Image Composites in Google Earth Engine for Improved Landslide Visibility: A Case Study of a Glacial Landscape. *Remote Sensing*. 14, 2301. doi:10.3390/rs14102301

Lithium Statistics and Information, 2025. https://www.usgs.gov/centers/national-minerals-information-center/lithium-statistics-and-information (10 May 2025)

Mwaniki, M., Moeller, M., Schellmann, G., 2015: A comparison of Landsat 8 (OLI) and Landsat 7 (ETM+) in mapping geology and visualising lineaments: A case study of central region Kenya, *Int. Arch. Photogramm. Remote Sens. Spatial Inf. Sci.*, XL-7/W3, 897–903. https://doi.org/10.5194/isprsarchives-XL-7-W3-897-2015

Sabins F.F., 1999: Remote sensing for mineral exploration. *Ore geology reviews*. 14.3-4, 157-183. doi:10.1016/s0169-1368(99)00007-4

S2 Applications, 2025. https://sentiwiki.copernicus.eu/web/s2-applications (10 May 2025)

Wang, G., Du, W., Carranza, E.J.M., 2017: Remote sensing and GIS prospectivity mapping for magmatic-hydrothermal base-and precious-metal deposits in the Honghai district, China. *Journal of African Earth Sciences*. 97–115. http://doi.org/10.1016/j.jafrearsci.2016.06.020

Zhao Q., Yu L., Li X., Peng D., Zhang Y., Gong P., 2021: Progress and Trends in the Application of Google Earth and Google Earth Engine. *Remote Sensing*. 13, 3778. doi:10.3390/rs13183778